EARTH SCIENCES
RESEARCH JOURNAL
Earth Sci. Res. J. Vol. 29, No. 2 (June, 2025): 211 - 218

UNIVERSIDAD NACIONAL DE COLOMBIA

GEOLOGICAL HAZARDS

The influence of vertical coastal land movement on relative sea level rise: a case study of Shanghai, China

Beining Wen[1], Miao Yu[2], Chong Liu[3], Yan Jiao[4]*, Qihang Kai[5]

1. College of Urban and Environmental Sciences, Northwest University, Xi'an 710127, Shaanxi, China
2. Shandong Xinhui Construction Group Co., LTD, Dongying 257901, Dongying, Shandong, China
3. School of Economics & Management , Northwest University, Xi'an 710127, Shaanxi, China
4.Mobile Postdoctoral Research Station of Public Administration, Northwest UniversityPos , Northwest University, Xi 'an Shaanxi 710127, China
5. Xi'an City Planning & Design institute, No. 178 South Laodong Road, Xi'an 710082, Shaanxi, China
*Corresponding author: jiaoyan@nwu.edu.cn

ABSTRACT

Understanding the current Vertical Land Motion (VLM), including subsidence or uplift, is the basis for projecting Relative Sea Level Rise (RLSR) and estimating related risks. However, in Shanghai, the impacts of the spatiotemporal change of VLM are little known. The purpose of this study was to quantify the impact of VLM on RSLR and investigate the spatiotemporal evolution characteristics of VLM through tide gauge records, satellite altimetry observations, and Interferometric Synthetic Aperture Radar (InSAR) measurements. The calculations indicated that the RSLR (5.67±0.58 mm/year) from 1969 to 2019 was approximately twice the SLR trend (2.44±0.28 mm/year) from 1993 to 2019. The VLM, especially subsidence, is the main driver of RSLR. Moreover, spatial and temporal patterns of VLM are highly uneven and nonlinear. These results reveal that VLM is the main driver of RSLR. Unfortunately, previous studies have mostly underestimated or overlooked the impact of VLM on the risks of RSLR and subsequent coastal flooding. Thus, prevention strategies for controlling VLM are warranted to minimize the negative impact related to the RSLR. Our research provides a theoretical basis for urban disaster prevention in Shanghai and the planning of coastal cities worldwide.

Keywords: Relative sea level rise; Vertical land motion; Shanghai; InSAR.

Influencia del movimiento vertical de la tierra en zonas costeras sobre el aumento relativo del nivel del mar: estudio de caso en Shanghái, China

RESUMEN

Comprender el movimiento vertical de la tierra (VLM) actual, incluida la subsidencia y la elevación, es la base para proyectar el aumento relativo del nivel del mar (RLSR) y estimar los riesgos relacionados. Sin embargo, en Shanghái, los impactos del cambio espaciotemporal del VLM son poco conocidos. El propósito de este estudio fue cuantificar el impacto del VLM en el RSLR e investigar las características de evolución espaciotemporal del VLM a través de registros de mareógrafos, observaciones de altimetría satelital y mediciones del Radar Interferométrico de Apertura Sintética (InSAR). Los cálculos indicaron que el RSLR (5,67 ± 0,58 mm/año) de 1969 a 2019 fue aproximadamente el doble de la tendencia del SLR (2,44 ± 0,28 mm/año) de 1993 a 2019. El VLM, especialmente la subsidencia, es el principal impulsor del RSLR. Además, los patrones espaciales y temporales del VLM son altamente desiguales y no lineales. Estos resultados revelan que el VLM es el principal impulsor del RSLR. Desafortunadamente, estudios previos han subestimado o pasado por alto, en su mayoría, el impacto de la VLM en los riesgos de RSLR y las subsiguientes inundaciones costeras. Por lo tanto, se justifican estrategias de prevención para controlar la VLM a fin de minimizar el impacto negativo relacionado con la RSLR. Nuestra investigación proporciona una base teórica para la prevención de desastres urbanos en Shanghái y la planificación de ciudades costeras en todo el mundo.

Palabras clave: Aumento relativo del nivel del mar; movimiento vertical de la tierra; Shanghái; Radar Interferométrico de Apertura Sintética

Record
Manuscript received: 15/12/2024
Accepted for publication: 18/05/2025

How to cite this item:
Wen, B., Yu, M., & Kai, Q. (2025). The influence of vertical coastal land movement on relative sea level rise: a case study of Shanghai, China. *Earth Sciences Research Journal, 29*(2), 211-218 https://doi.org/10.15446/esrj.v29n2.118098

1. Introduction

Sea level rise is a crucial index of climate change. And it is accelerating due to melting from the ice sheet and glaciers and the thermal expansion of ocean water (Horton et al., 2018; Jevrejeva et al., 2016). In situ and remote sensing data show that the rate of global sea-level rise over the past two centuries has increased at faster rates than in the last two or three millennia (Vermeer and Rahmstrof, 2009; Kemp et al., 2011). And the Intergovernmental Panel on Climate Change (IPCC) highlighted that the rate of mean global Sea Level Rise (SLR) had been up from 1.4 mm/year (1901-1990) to 3.6 mm/year (2006-2015) (IPCC, 2019). As a result, the global mean sea level is projected to range from 0.5 m to 1.2 m by the end of the 21st century, exacerbating flood risks and persisting till the next century, with significant impacts on coastal socio-economic, natural environment and ecosystems (Kopp et al., 2014).

Regional sea-level rise significantly varies worldwide, mainly due to the different situations of Vertical Land Motion (VLM) in local areas (Pörtner et al., 2019), especially in coastal delta regions (Nicholls et al., 2021). The Relative Sea Level Rise (RSLR) has been proposed to refer to the elevation difference between mean sea level and land surface (Nicholls et al., 2021; Rovere et al., 2016), which can be defined as the sum of local VLM and SLR. The VLM includes subsidence or uplift, due to natural processes (e.g., Glacial Isostatic Adjustment (GIA), sediment compaction, and tectonics) and anthropogenic processes (e.g., groundwater extraction and land-use change) (Higgins, 2016; Minderhoud et al., 2016; Shirzaei et al., 2021; Yuill et al., 2009). Land subsidence has been identified as the main pattern of VLM (Dokka, 2006; Gómez et al., 2021). Because of the rapid sediment compaction and deposit, coastal delta regions are experiencing a faster rate of land subsidence than global SLR (Minderhoud, 2019; Tessler et al., 2018). In addition, due to the abundance of coastal urban deltas, rapid urbanization, and dense population of coastal cities, RSLR is growing faster than in other regions, especially in developing Asia (Hallegatte et al., 2013; Nicholls et al., 2021), and VLM could be the primary driver to RSLR over the 21st century (Cao et al., 2021; Fuchs, 2010; Nicholls et al., 2021). For example, as one of the biggest coastal cities around the world with exceeding 11 million citizens in 2020 and an expected population of up to nearly 36 million people by 2030 (Razvadauskas, 2019), Jakarta has shown that the land subsidence rate is up to 60 times faster than SLR. Moreover, it has been estimated that land subsidence could be responsible for about 88% contribution to coastal flood risks by 2050 (Takagi et al., 2016a & b).

For many coastal cities in Asia, understanding local VLMS is important to guide the decision-making process for coastal mitigation and adaptation plans to address serious future threats. Over the last decade, RSLR and flood hazards in Shanghai have received much attention. For example, by simulating the consequence of the interaction of land subsidence, SLR, and storm surges, Wang et al. (2012) found that Shanghai is sinking, and the maximum rate of subsidence is 24.12 mm/year. The result stresses that severe land subsidence is the primary driver causing RSLR and flooding risks, which will further reduce the effectiveness of dikes by decreasing their height. Yin et al. (2013) characterized the combined contribution of SLR and land subsidence to fluvial flooding in the Huangpu River in Shanghai. The analysis shows that land subsidence results in floods becoming more common than before. Cheng et al. (2018) provided a map of RSLR behaviors over the past decades. They declares the local land subsidence rate has been approximately 5 mm/year since 2004, mainly causing RSLR.

To provide accurate and comprehensive measurements of VLM, more and more studies have used space-borne methods, such as Global Navigation Satellite System (GNSS) and Interferometric Synthetic Aperture Radar (InSAR) (Hu et al., 2019; Yin et al., 2019; Yu et al., 2017). Among these methods, interferomet-ric synthetic aperture radar (InSAR) technology can extract small deformation information of the surface, and has the characteristics of small weather influence, large coverage area, low cost and high measurement accuracy, which makes up for the shortcomings of traditional deformation monitoring. It has been applied in many urban land subsidence monitoring. For example, Yu et al. (2017) applied Differential Synthetic Aperture Radar Interferometry (DInSAR) approach to analyze the VLM for 2015-2016. And the highest land subsidence rate of 30 mm/year has been measured. In addition, Yin et al. (2019) estimated coastal flood hazards evolving SLR and land subsidence in Lingang New City in Shanghai using the DInSAR technique. The results show that combing the contribution of land subsidence, RSLR is projected to be 0.11 m and 0.23 m by 2030 and 2050, respectively. These rises would extend the flooding area by nearly 6% and 15% by 2030 and 2050, separately, for 100-year flooding.

Therefore, this study takes Shanghai, China as an example, and uses InSAR analysis, the most advanced VLM measurement method, to study the time series of Shanghai VLM, and discusses how VLM, especially land subsidence, changes and affects RSLR. Then give a new view on the flood disaster in coastal cities.

2. Materials and methodology

2.1. Study area

Shanghai is a coastal city that has 213 km of coastlines. It is located between 30°40'~31°53' north latitude and 120°51'~122°12' east longitude. Shanghai is bounded by the East China Sea to the east, Jiangsu Province to the northwest, Zhejiang Province to the southwest, Hangzhou Bay to the south, and the Yangtze River to the north and Jiangsu Province. In addition to the hilly landform in the southwest part of the region, most of the region is low and flat, with an average elevation of about 4m, and the elevation of the urban area is less than 3m, which is seriously lower than the high water level of the Huangpu River. Shanghai is a typical subtropical monsoon climate, with relatively humid climate and distinct four seasons. The average annual temperature is about 15.8°C, and the average annual rainfall can reach 1191mm. The rainfall distribution is uneven in different seasons, generally showing the characteristics of more rainfall in spring and summer, less in autumn and winter, and the rainfall is mostly concentrated in the flood season from May to September. At the same time, heavy rainfall and high tide events are easy to occur during flood season and typhoon, which will cause river basin floods and huge economic losses (Xian et al., 2018). And the resident population was over 23 million in 2020 from the 6th National Population Census of China, almost 1.5 times that of 10 years ago. Urban construction is developing rapidly, including the reconstruction of old areas, new residential areas, a large number of dense high-rise and super-high-rise buildings, and the development and utilization of underground space. The vigorous development of urban construction activities in Shanghai, especially the rapid development of underground space, has a serious impact on land subsidence. (Shen and Xu 2011). By the end of 2019, the construction area of houses with more than eight stories has increased from 9.59×106 m^2 in 1990 to 4.96×108 m^2. In some areas, the settlement of shallow soft soil caused by urban construction accounts for a considerable proportion of the total settlement. Geological experts pointed out that in the current construction boom, engineering construction activities have become the main cause of land settlement.

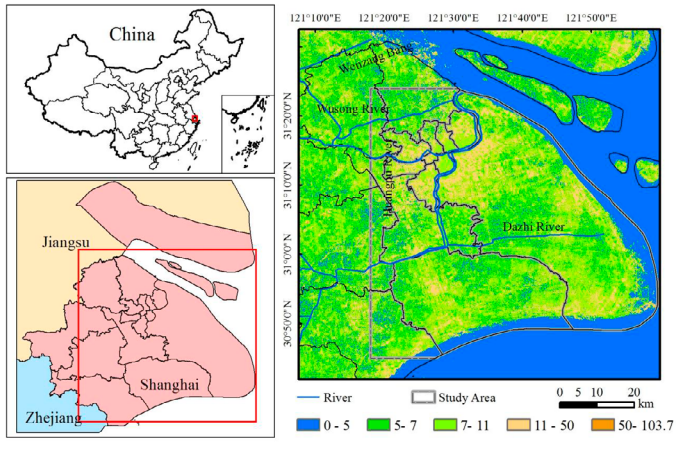

Figure 1. Location of the Shanghai city

2.2. Research Method

Figure 2 illustrates the procedural steps involved in conducting InSAR analysis to measure local Vertical Land Motion (VLM). Firstly, the selected pairs

of Single Look Complex (SLC) SAR scenes were individually co-registered using orbit information obtained from a 1-arc sec Shuttle Radar Topography Mission (SRTM) Digital Elevation Model (DEM), thereby leveraging the phase difference between the acquisitions (Farr et al., 2007). The Enhanced Spectral Diversity (ESD) approach was employed to improve the quality of each co-registration.

Subsequently, a series of interferograms were generated by multiplying the reference scene with the complex conjugate of the secondary scene, utilizing the co-registered data. The resulting interferometric phase represented the phase difference between the two acquisition dates (Gens and Van Genderen, 1996). During this step, the flat-earth and topographic phases were subtracted based on the metadata information from orbital records and the 1-sec arc STRM DEM, respectively.

To reduce inherent speckle noise and enhance interpretability, a multi-looking operator was applied to each image. Furthermore, a Goldstein Phase Filter, utilizing Fast Fourier Transformation (FFT), was implemented to mitigate noise resulting from temporal and geometric decorrelation, volume scattering, and other processing errors. Consequently, a total of 24 interferograms were generated for the period spanning 2015 to 2020 up to this stage of the analysis.

To identify high-quality pixels with reduced noise, only those with an average coherence exceeding 0.2 were considered for subsequent analysis. Each interferogram's phase had to be unwrapped to establish a relationship between the interferometric phase and the corresponding topographic height. Therefore, the unwrapping process was carried out individually for each interferogram using a minimum cost-flow algorithm facilitated by SNAPHU. The unwrapped phase was then converted from radians into absolute displacements. Geocoding was applied to all datasets to accurately determine the geographic location of the selected high-quality pixels.

To minimize the influence of orbital errors and atmospheric delays, the single geocoded displacement products from 2015 to 2020 were stacked in chronological order. This stacking process facilitated the generation of a time series depicting the line-of-sight (LOS) deformation. It is important to note that, for the purposes of this study, the LOS deformation rate obtained through linear fitting was excluded to focus solely on uncovering the spatial and temporal evolution patterns of VLM.

2.3. Research Data

2.3.1. Relative sea level rise data

Tide gauge records serve as the primary data source for assessing coastal relative sea level changes over the past century. These records measure the local Relative Sea Level (RSL), which refers to the vertical distance between sea level and the land where tide gauge stations are situated (Restrepo-Ángel et al., 2021). In this study, monthly RSL data from 1969 to 2019 were obtained from the Lusi tide gauge station, the closest station to Shanghai, through the Permanent Service for Mean Sea Level (PSMSL, https://www.psmsl.org/data/obtaining/). The selected period was based on the availability of the longest time series data from the Lusi tide gauge station. Harmonic analysis was applied to these data to determine tidal constituents, significant tidal statistics, and their respective amplitudes and phases. To account for missing data, which constituted 92% of the dataset, interpolation was performed using harmonic analysis.

To eliminate seasonal variability from the RSL data, the climatological monthly mean was subtracted from the monthly values. Yearly averaged records were then calculated based on the monthly data. The least-squares linear fitting method was employed to estimate the trend of Relative Sea Level Rise (RSLR) using the RSL datasets spanning the period from 1969 to 2019. By considering a 50-year timeframe, the RSLR trend was calculated based on the tide gauge records, aiming to minimize the influence of inter-annual and decadal signals.

2.3.2. Sea Level Rise Data

In recent years, satellite altimetry data have emerged as a valuable tool for accurately assessing absolute sea level changes in numerous coastal regions (Nerem et al., 2018; Restrepo-Ángel et al., 2021). For this study, monthly sea level data covering the period from 1993 to 2019 were obtained from the National Oceanic and Atmospheric Administration (NOAA) Laboratory for Satellite Altimetry, specifically from the Yellow Sea area, which encompasses the study region (https://www.star.nesdis.noaa.gov/socd/lsa/SeaLevelRise/). These data are derived from the records collected by multiple satellite radar altimeters, including TOPEX/Poseidon (T/P), Jason-1, Jason-2, and Jason-3, ensuring a comprehensive time series spanning from 1993 to 2019.

To ensure accuracy, the seasonal variability was meticulously eliminated from the sea level data, and the impacts of Glacial Isostatic Adjustment (GIA) on the geoid were excluded by the NOAA Laboratory for Satellite Altimetry. Additionally, the local Sea Level Rise (SLR) trend was determined using the least-squares linear fitting method, providing a robust assessment of sea level changes in the study area.

2.3.3. Vertical land motion data

To date, only a limited number of studies have examined Vertical Land Motion (VLM) using InSAR analysis, with a focus on short time series (less than 4 years) or specific areas within the Shanghai region (Ye et al., 2016; Yin et al., 2015, 2019; Zhao et al., 2015, 2019). Consequently, there is a dearth of knowledge regarding the spatiotemporal variability characteristics of VLM in the study area. To address this research gap, the present study employed InSAR analysis, a cutting-edge method for measuring VLM with exceptional precision, utilizing Sentinel-1A datasets spanning the period from 2015 to 2020.

Table 1. Sentinel-1A data in ascending orbit, frame 97 and path 171

Year	Acquisition dates
2015	1 Aug, 29 Nov
2016	12 Jan, 4 Mar, 15 May, 19 Aug, 18 Oct, 17 Dec
2017	3 Feb, 4 Apr, 27 June, 7 Sep, 18 Nov
2018	17 Jan, 18 Mar, 29 May, 9 Aug, 25 Nov
2019	24 Jan, 13 Mar, 24 May, 4 Aug, 15 Oct, 26 Dec
2020	31, Jan

The SAR scenes captured by the Sentinel-1A satellite were obtained from the Alaska Satellite Facility Distributed Active Archive Center, which processes Copernicus Sentinel data on behalf of the European Space Agency (ASF DAAC, https://search.asf.alaska.edu), covering the period from August 2015 to January 2020. Although both ascending and descending orbits were available for Sentinel-1A, this study focused exclusively on 25 scenes from the ascending orbit track. This selection was made because the ascending orbit track provided a longer time series dataset for the study area, as demonstrated by Potin et al., 2016 (Table 1). The generation of interferograms and subsequent phase unwrapping were performed using the Sentinel Application Platform (SNAP) software and the Statistical-Cost Network-Flow Algorithm for Phase Unwrapping (SNAPHU) algorithm, respectively (Chen & Zebker, 2001, 2002).

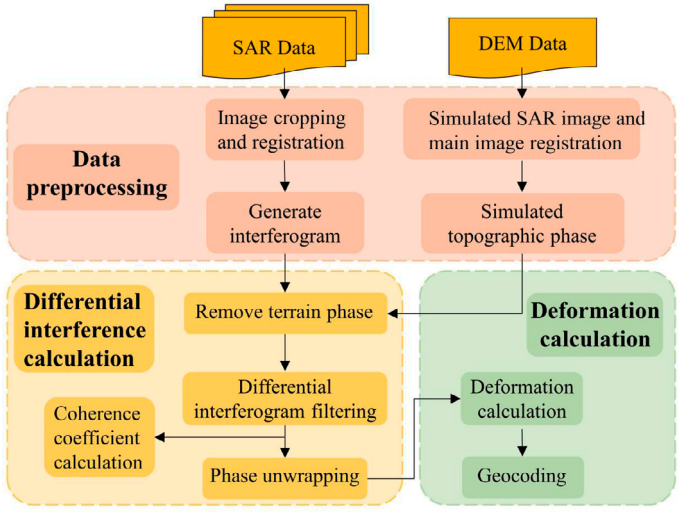

Figure 2. Flow diagram of InSAR analysis (modified from Gómez et al., 2021; Li et al., 2018)

3. Results

3.1 Sea level rise and Relative sea level rise

Monthly sea level change data were collected from multiple satellite radar altimeters from 1993-2019, which indicates an increasing trend of about 2.44±0.28 mm/year for the offshore area of Shanghai (Fig. 3). The absolute sea level rise is mainly caused by natural factors such as melting of glaciers and ice sheets and thermal expansion of temperature.

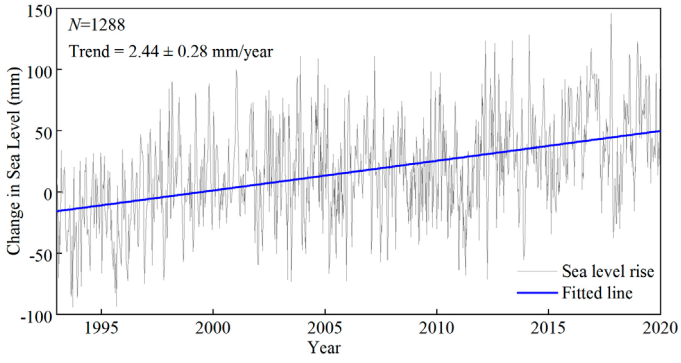

Figure 3. Time series of sea level rise from 1993 to 2019. Sea level rise plot generated by Matlab 2021a (https://www.mathworks.com/products/matlab.html)

Relative sea level change is a general term for the rise (or fall) of sea level relative to the land surface (or underlying primordial sedimentary surface). This movement can be the rise and fall of the sea level itself, the rise and fall of the land surface or the underlying sediment surface, or both occur at different magnitudes. Hence, relative sea level rise (RSLR) is the result of the joint action of natural and human factors (Fig. 4), the main factors are climate, ocean, geological environment, resource exploitation, man-made engineering construction, etc., which induces a series of resource, environmental, economic and social problems and risks, endangering the urbanization construction and economic and social development of coastal areas. However, monthly relative sea level data were obtained from the Lusi tide gauge station from 1969 to 2019, and the results show 5.67±0.58 mm/year trend for RSLR (Fig. 5). The trend value of RSLR in Shanghai is twice faster than SLR. This means that SLR, induced by the melting of glaciers and ice sheets as climate change, represents less than half of the contribution for RSLR. Hence, what can be concluded from this result is that significant differences between RSLR and SLR are most likely owing to the impact of local Vertical land motion (VLM) on the RLSR (Abidin et al., 2011; Eggleston & Pope, 2013; Ingebritsen and Galloway, 2014).

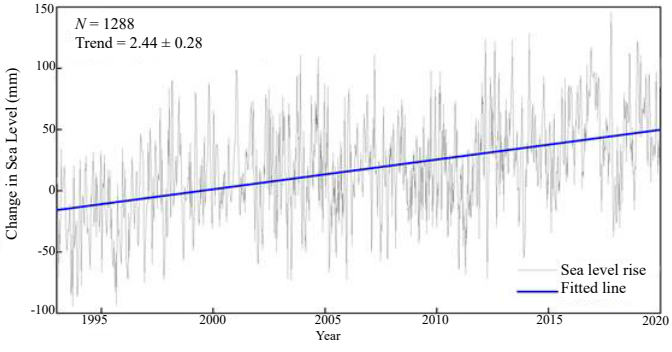

Figure 4. Diagram of relative sea level rise and its effects

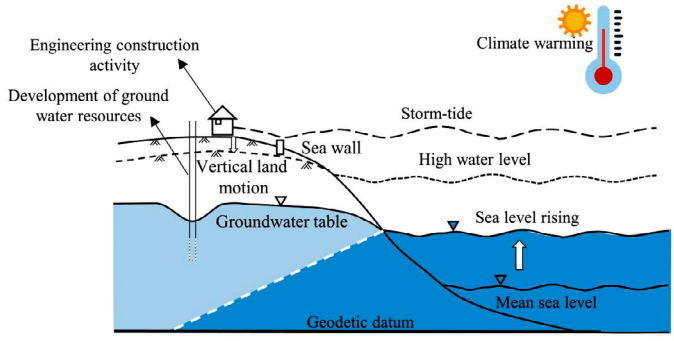

Figure 5. (a)Time series of relative sea level rise from 1969-2019. Blue dashed line, and solid line separately refers to the monthly and yearly relative sea level change. (b) Linear fit of relative sea level rise trends for 1969-2019. Relative sea level rise plots generated by Matlab, 2021a (https://www.mathworks.com/products/matlab.html)

3.2 Vertical land motion

This study applied the InSAR analysis technique to measure the VLM from 2015-2020 based on the Sentinel-1A ascending orbit track datasets. The deformation map was generated and shown in Figure 5. The scale of displacements corresponds to LOS in units of the centimeter.

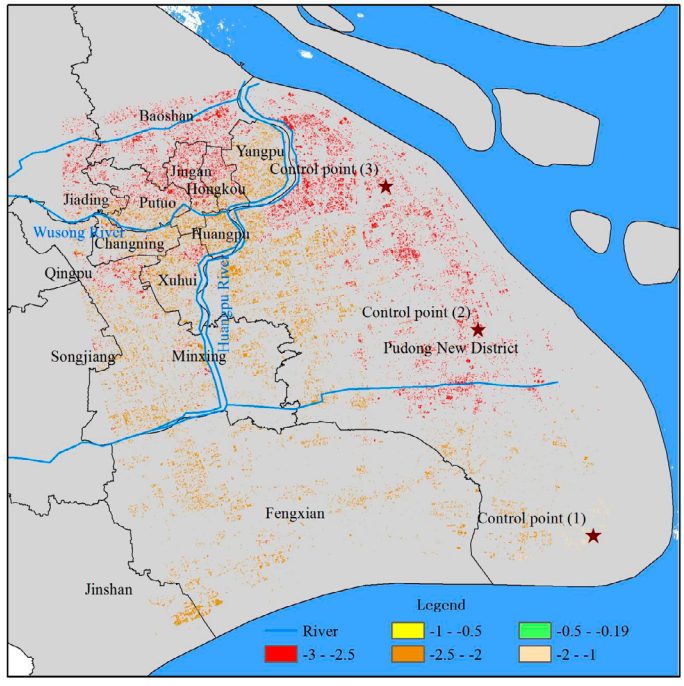

Figure 6. The map of VLM from 2015-2020 using the InSAR analysis technique on Sentinel-1A data sets.

In the study area, the InSAR analysis results reveal a wide range between -3 cm and -0.19 cm of VLM in Shanghai (Fig. 5). The largest VLM during the 2015-2020 period is up to -3 cm in the northeastern area of Shanghai. In contrast, in south Shanghai, the land displacements show slight uplift or subsidence (Fig. 5a). It is worth highlighting that the values of the VLM in the study area unevenly distribute on the spatial change pattern, The VLM in the western area of the Huangpu River shows severe subsidence between 2.5 cm

and 3 cm. On the east part of the Huangpu River, land subsidence decreases to less than 2.5 cm, and a slight uplift or sink can be observed in the southwestern coastline. and land subsidence increases in the northern direction. The time series of LOS displacements for selected three locations show high nonlinear evolution characteristics (Fig. 5b). These displacements of sites exhibit apparent fluctuations during the 2015-2018 period and have become stable since 2018.

4. Discussion

4.1 The contribution of two components to relative sea level rise

Since VLM and SLR are the main components of RSLR, understanding the quantitative contribution of these two parts is essential to projecting the RSLR scenarios and potential coastal flood risks in the future. However, even though existing studies in Shanghai highlighted the significance of RSLR, the quantitative assessment of contribution from RSLR and SLR has not been conducted (Wang et al., 1995; Chen, 1991; Yan et al., 2016). This study calculated the long-term trends of RSLR and SLR through tide gauge records and satellite altimetry observations, respectively. The rate of RSLR in Shanghai is 5.67±0.58 mm/year from 1969 to 2019, which is over twice faster than the SLR rate of 2.44±0.28 mm/year during 1993-2019. This means that SLR, induced by the melting of glaciers and ice sheets as climate change, represents less than half of the contribution for RSLR, and in contrast, VLM is the main driver of RSLR. Unfortunately, previous studies mostly underestimated or even overlooked the impact of VLM on risks of RSLR and subsequential coastal flooding (Lv et al., 2021; Wang et al., 2018; Yin et al., 2021). We believe our results fill a gap in the quantitative analysis of SLR and VLM contributions, which reveal the evidence that RSLR is much more affected by VLM than SLR. Therefore, if VLM can be controlled or stopped through local measures, RSLR will be reduced, mitigating the harm of coastal flooding.

4.2 Evolution characteristics of vertical land motion

In Shanghai, the main pattern of VLM over the 2015-2020 period shows subsidence in most areas. Still, only a tiny space showed slight uplift in the southwest, most likely due to the impacts of GIA and artificial recharge to ground acquire (Peltier et al., 2015; Zhang et al., 2015). For the VLM time series of 6 years, natural-induced deformation (e.g., GIA, sediment compaction, and tectonics) is assumed negligible because the ground change by natural processes can only be measured in the long-term period in the Holocene era (Shirzaei and Bürgmann, 2018; Xue et al., 2005). Additionally, there are no localized characteristics with the rapid and sudden settlement rate due to the contemporary depletion of aquifers and reservoirs, and earthquakes. Thus, this study indicates anthropogenic activities as the main factor for local VLM from 2015-2020.

The map of VLM reveals the uneven distribution in the study area (Fig. 6). The wide range of displacements is approximately between –4 cm and 1.7 cm. Almost certainly, this pattern is induced by the impacts of groundwater overdraft and additional load from building construction (Chai et al., 2004; Xu et al., 2016). The VLM settlement in the west of the Huangpu River is higher than that in the east of the Huangpu River. This uneven distribution of VLM values relates to the uneven distribution of residents and human activities and urbanization. Specifically, the west side of the Huangpu River, called the Puxi Area, has developed over hundreds of years, and citizens and infrastructures are intensely concentrated there. In contrast, to meet the increasing demand for land and natural resources by rapid urbanization, Pudong New Area, located in the eastern Huangpu River, has only seen rapid development in a few decades. Thus, human activities in Pudong New Area are less than those in Puxi Area, and the VLM in the former was relatively lighter than the latter. The Lingang New Area, located in the southeastern part of Shanghai along the coastline, has been planned for development in recent years. As the newest developing area, Lingang New Area is experiencing the slightest subsidence compared with other parts.

The time series of displacements for selected three locations show high nonlinear evolution characteristics (Fig. 7). These displacements exhibit apparent fluctuations during the 2015-2018 period and become likely stable since 2018, probably thanks to the local government introducing a series of policies for groundwater extraction controlling and construction standards (Wang et al., 2012; Xu et al., 2012; Ye et al., 2016). However, in recent memory of studies in Shanghai, the rates of VLM were assumed linear and would continue to the future scenarios by 2050 and 2100 (Wang et al., 2018; Yin et al., 2013, 2020, 2021). This kind of assumption based on no significant change in groundwater exploitation overlooked the temporal evolution pattern due to land subsidence controlling measures in VLM, leading to VLM scenarios would be overrated or underrated. Indeed, a range of evidence reveals that the proper strategies for groundwater extraction and building construction can positively control and even stop local land subsidence. For example, in Japan, land subsidence became a significant problem during the 20th century due to excessive groundwater withdrawal. To combat this issue, a series of controlling measures were implemented, including groundwater pumping control, surface water development, and groundwater recharge to manage the water resources more effectively and prevent excessive extraction of groundwater (Cao et al., 2021; Esteban et al., 2020). As a result, the subsidence condition in Japan has been almost halted. Similarly, the Netherlands and the United States have also dealt with land subsidence and implemented measures to mitigate its effects successfully. (Holzer and Johnson, 1985; Koster et al., 2018).

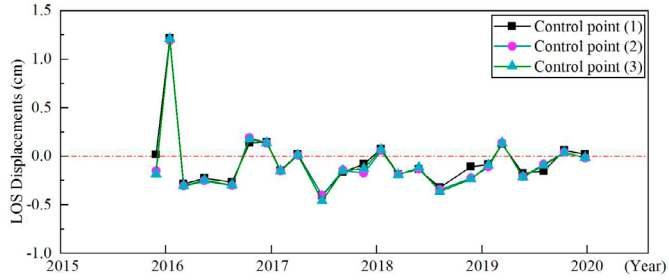

Figure 7. Time series of LOS displacements (cm) at selected control points for the 2015-2020 period.

Previous studies applying linear extrapolation method to estimate land subsidence scenarios likely overestimated the future VLM conditions. As the major contribution to RSLR and coastal flood hazards, land subsidence rate could be retarded and even totally stopped as long as implementing effective controlling strategies by local decision-making, which would further decrease the potential threat from RSLR and coastal flooding. This result might provide some reference basic information for policy planning and relieve the public anxious emotion about future unpredictable risks. Furthermore, it would provide a new perspective of planning countermeasures to future coastal hazards from costly engineering constructions to applying practical effective groundwater management and water resources arrangement, which would reduce the local economic pressure and benefit city development.

4.3 Risk and its management

The composite flood disaster is a typical multi-disaster event caused by typhoon, storm surge, astronomical tide, heavy rainfall, sea level rise and land subsidence. Under the background of climate change and rapid urbanization in the past few decades, flood disasters caused by typhoon storm surge, extreme rainfall and relative sea level rise have become the most common and most serious natural disasters in coastal cities (Adelekan, 2010; Fang et al., 2017; Du et al., 2019). Coastal cities are extremely sensitive to sea level rise, and sea level rise and changes in coastal water depth will increase the risk of coastal flooding, while land subsidence caused by rapid urbanization will cause relative sea level rise, resulting in the "amplification effect" of flood disaster (Wang et al., 2018). As one of the global financial centers and the largest city in China, Shanghai is also one of the megacities with the highest risk of coastal flooding in the world (Balica et al., 2012; Ridder et al., 2020). Under the complex background of global warming and sea level rise, Shanghai faces severe flood risk prevention pressure, and its flood disasters are mainly urban waterlogging caused by extreme rainfall and coastal flooding caused by extreme typhoon storm surge (Yang et al., 2021). Human activities, land subsidence, sea level rise and extreme climate events will further increase the risk of composite flood disaster in Shanghai. Located in the delta front of the Yangtze River estuary, Shanghai is low-lying and extremely sensitive to sea level rise (Fig. 8). Due to the combined influence of typhoons, storm surges, heavy rainfall and river floods, disasters in this region have the characteristics of "wind, storm, tide and flood", which easily lead to the "amplification effect" caused by disaster confluence and disaster superposition (Muis et al., 2016).

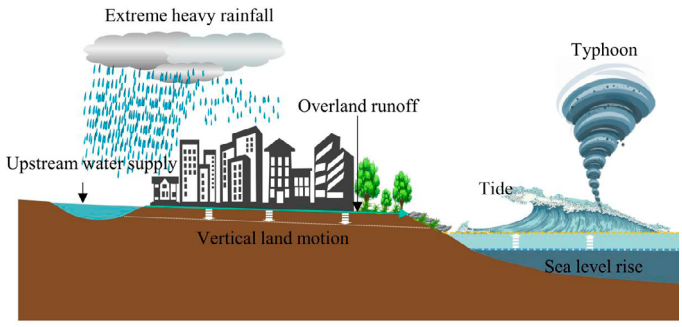

Figure 8. Conceptual model of compound flood disaster event in coastal cities

The problem of land subsidence in Shanghai began in 1921. After the formation of modern industrial zone, unreasonable groundwater exploitation caused land subsidence in the downtown area of Shanghai. Since 1956, Shanghai has taken a series of measures to deal with land subsidence. Since the mid-1960s, Shanghai has developed an annual water harvesting and irrigation program. Especially since the 1970s, the central urban area of Shanghai has basically realized effective control over the ground. In the 1990s, as Shanghai began to implement market economic reform, it ushered in a new round of development opportunities. With the influx of a large number of people into Shanghai and the large-scale urban construction, the demand for urban water resources and engineering geological activities are increasing day by day, and the ground in Shanghai has obvious vertical movement phenomenon compared with the earlier period. In 2013, Shanghai was hit by Typhoon Fitow, which caused a record water level in the upper reaches of the Huangpu River under the combination of storm surge floods, which caused a great impact on the flood control and drainage infrastructure.

In general, the interaction of sea level rise, land subsidence, typhoon storm surge, extreme rainfall and other disaster-causing factors leads to frequent flooding disasters in coastal cities, resulting in great social and economic losses. In order to cope with the extreme typhoon storm surge event in Shanghai, it can be chosen to add the tide gate of Huangpu River, and raise the flood control wall behind the gate 2 m to prevent river flooding. For extreme rainfall events, overall drainage improvements, the use of deep underground tunnels, the addition of permeable pavements and green roofs, and a combination of these measures can be taken. The biggest feature of gray engineering measures is high flood control efficiency and large capacity, but the disadvantage is that it is not friendly to the environment, and blue and green non-engineering measures can make up for this deficiency. According to the actual situation of Shanghai, the strategy to deal with the combined flood disaster still needs to focus on gray engineering measures, and constantly strengthen the attention and investment of blue and green non-engineering measures.

4.4 Uncertainty and limitation

To minimize the inter-annual impact and measuring error, this study employed long-term RSLR and SLR data. Even so, there are still uncertainties about RSLR and SLR due to local climate variability, record length, and record failures. Additionally, the tide gauge station used in estimating the RSLR trend is not located in the Shanghai leading to uncertainties of consequences.

There are certain limitations in terms of VLM measurement, because the SAR datasets were only obtained from Sentinel-1A ascending orbit track. Therefore, to provide more comprehensive and higher accurate long-term measurements of VLM, multi-temporal and multi-platform (including ascending and descending orbits) SAR datasets should be applied in the following studies.

5. Conclusion

This study demonstrates the quantitative contributions of SLR and VLM to RSLR in Shanghai through long-term data analysis. Furthermore, it investigates the spatiotemporal evolution characteristics of local VLM applying state–of–the–art InSAR analysis technique. Based on the results of this study, two conclusions can be drawn.

1. The RSLR of 5.67±0.58 mm/year over the 1969-2019 period is approximately over twice than SLR trend of 2.44±0.28 mm/year during the 1993-2019 period, which shows that the VLM in Shanghai, particularly land subsidence, is likely to be the main driver for accelerating RSLR and exacerbating related coastal risks
2. Spatial and temporal change patterns of VLM are highly uneven and nonlinear. As a result, linear assumptions of the VLM trend, especially land subsidence, used in previous studies would overestimate the future RSLR scenarios and the loss of future coastal hazards. Therefore, it is clear that local government should propose VLM controlling policies because the longer this problem continues, the more expensive any future adaptation strategies will be.
3. Although we have verified the experimental results with the previous results of other researchers, it is necessary to carry out field operations to obtain the actual data of surface deformation. Combining traditional methods with InSAR technology will obtain more accurate and reliable experimental results. In addition, accurately determining the vertical land movement of coastal cities and improving our robust prediction of coastal vulnerability to sea level rise can build a more comprehensive geological disaster prevention and control system for coastal cities, which will be the entry point for subsequent research.

Conflicts of Interest:

The authors declare no conflict of interest.

Funding

This research is supported by Soft Science Research Project of Shaanxi Province "Research on the Principal-agent Mechanism for the Whole-people Ownership of Natural Resource Assets in Qinling National Park"(2023-CX-RKX-109) and Shaanxi Provincial Education Department "Research on the Legal Framework for Eco-space Governance in the Yellow River Basin of Shaanxi Province"(23JK0228).

References

Abidin, H. Z., Andreas, H., Gumilar, I., Fukuda, Y., Pohan, Y. E., & Deguchi, T. (2011). Land subsidence of Jakarta (Indonesia) and its relation with urban development. Natural Hazards, 59(3), 1753–1771. https://doi.org/10.1007/s11069-011-9866-9

Adelekan I O. (2010). Vulnerability of poor urban coastal communities to flooding in Lagos, Nigeria. Environment and Urbanization, 22, 433-450. https://doi.org/10.1177/0956247810380141

Balica S F, Wright N G, Van Der Meulen F. (2012). A flood vulnerability index for coastal cities and its use in assessing climate change impacts. Natural Hazards, 64: 73-105. https://doi.org/10.1007/s11069-012-0234-1

Cao, A., Esteban, M., Valenzuela, V. P. B., Onuki, M., Takagi, H., Thao, N. D., & Tsuchiya, N. (2021). Future of Asian Deltaic Megacities under sea level rise and land subsidence: Current adaptation pathways for Tokyo, Jakarta, Manila, and Ho Chi Minh City. Current Opinion in Environmental Sustainability, 50, 87–97. https://doi.org/10.1016/j.cosust.2021.02.010

Chai, J.-C., Shen, S.-L., Zhu, H.-H., & Zhang, X.-L. (2004). Land subsidence due to groundwater drawdown in Shanghai. Geotechnique, 54(2), 143–147. https://doi.org/10.1680/geot.2004.54.2.143

Chen, C. W., & Zebker, H. A. (2001). Two-dimensional phase unwrapping with use of statistical models for cost functions in nonlinear optimization. JOSA A, 18(2), 338–351. https://doi.org/10.1364/JOSAA.18.000338

Chen, C. W., & Zebker, H. A. (2002). Phase unwrapping for large SAR interferograms: Statistical segmentation and generalized network models. IEEE Transactions on Geoscience and Remote Sensing, 40(8), 1709–1719. https://doi.org/10.1109/TGRS.2002.802453

Chen Xiqing. (1991). Sea-level changes since the early 1920's from the long records of two tidal gauges in Shanghai, China. Journal of Coastal Research, 787–799. https://www.jstor.org/stable/4297894

Cheng, H. Q., Chen, J. Y., Chen, Z. J., Ruan, R. L., Xu, G. Q., Zeng, G., Zhu, J. R., Dai, Z. J., Chen, X. Y., Gu, S. H., Zhang, X. L., & Wang, H. M. (2018). Mapping Sea Level Rise Behavior in an Estuarine Delta System: A Case Study along the Shanghai Coast. Engineering, 4(1), 156–163. https://doi.org/10.1016/j.eng.2018.02.002

Dokka, R. K. (2006). Modern-day tectonic subsidence in coastal Louisiana. Geology, 34(4), 281–284. https://doi.org/10.1130/G22264.1

Du S, Cheng X, Huang Q, et al. (2019). Brief communication: Rethinking the 1998 China floods to prepare for a nonstationary future. Natural Hazards and Earth System Sciences, 19(3): 715-719. https://doi.org/10.5194/nhess-19-715-2019

Eggleston, J., & Pope, J. (2013). Land subsidence and relative sea-level rise in the southern Chesapeake Bay region. US Geological Survey Circular, 1392, 30. https://dx.doi.org/10.3133/cir1392

Esteban, M., Takagi, H., Nicholls, R. J., Fatma, D., Pratama, M. B., Kurobe, S., Yi, X., Ikeda, I., Mikami, T., Valenzuela, P., & Avelino, E. (2020). Adapting ports to sea-level rise: Empirical lessons based on land subsidence in Indonesia and Japan. Maritime Policy & Management, 47(7), 937–952. https://doi.org/10.1080/03088839.2019.1634845

Fang J, Liu W, Yang S, et al. (2017). Spatial-temporal changes of coastal and marine disasters risks and impacts in Mainland China. Ocean & Coastal Management, 139: 125-140. https://doi.org/10.1016/j.ocecoaman.2017.02.003

Farr, T. G., Rosen, P. A., Caro, E., Crippen, R., Duren, R., Hensley, S., Kobrick, M., Paller, M., Rodriguez, E., & Roth, L. (2007). The shuttle radar topography mission. Reviews of Geophysics, 45(2). https://doi.org/10.1029/2005RG000183

Fuchs, R. J. (2010). Cities at Risk: Asia's Coastal Cities in an Age of Climate Change. 12.

Gens, R., & Van Genderen, J. L. (1996). Review Article SAR interferometry—Issues, techniques, applications. International Journal of Remote Sensing, 17(10), 1803–1835. https://doi.org/10.1080/01431169608948741

Gómez, J. F., Kwoll, E., Walker, I. J., & Shirzaei, M. (2021). Vertical Land Motion as a Driver of Coastline Changes on a Deltaic System in the Colombian Caribbean. Geosciences, 11(7), 300. https://doi.org/10.3390/geosciences11070300

Higgins, S. A. (2016). Review: Advances in delta-subsidence research using satellite methods. Hydrogeology Journal, 24(3), 587–600. https://doi.org/10.1007/s10040-015-1330-6

Hallegatte, S., Green, C., Nicholls, R. J., & Corfee-Morlot, J. (2013). Future flood losses in major coastal cities. Nature Climate Change, 3(9), 802–806. https://doi.org/10.1038/nclimate1979

Holzer, ThomasL., & Johnson, A. I. (1985). Land subsidence caused by ground water withdrawal in urban areas. GeoJournal, 11(3). https://doi.org/10.1007/BF00186338

Horton, B. P., Kopp, R. E., Garner, A. J., Hay, C. C., Khan, N. S., Roy, K., & Shaw, T. A. (2018). Mapping Sea-Level Change in Time, Space, and Probability. Annual Review of Environment and Resources, 43(1), 481–521. https://doi.org/10.1146/annurev-environ-102017-025826

Hu, B., Chen, J., & Zhang, X. (2019). Monitoring the land subsidence area in a coastal urban area with InSAR and GNSS. Sensors, 19(14), 3181. https://doi.org/10.3390/s19143181

Ingebritsen, S. E., & Galloway, D. L. (2014). Coastal subsidence and relative sea level rise. Environmental Research Letters, 9(9), 091002. https://doi.org/10.1088/1748-9326/9/9/091002

Jevrejeva, S., Jackson, L. P., Riva, R. E. M., Grinsted, A., & Moore, J. C. (2016). Coastal sea level rise with warming above 2 °C. Proceedings of the National Academy of Sciences, 113(47), 13342–13347. https://doi.org/10.1073/pnas.1605312113

Kemp, A.C.; Horton, B.P.; Donnelly, J.P.; Mann, M.E.; Vermeer, M.; Rahmstorf, S. (2011) Climate related sea-level variations over the past two millennia. Proc. Natl. Acad. Sci. 108, 11017–11022. https://doi.org/10.1073/pnas.1015619108

Kopp, R. E., Horton, R. M., Little, C. M., Mitrovica, J. X., Oppenheimer, M., Rasmussen, D. J., Strauss, B. H., & Tebaldi, C. (2014). Probabilistic 21st and 22nd century sea-level projections at a global network of tide-gauge sites. Earth's Future, 2(8), 383–406. https://doi.org/10.1002/2014EF000239

Koster, K., Stafleu, J., & Stouthamer, E. (2018). Differential subsidence in the urbanised coastal-deltaic plain of the Netherlands. Netherlands Journal of Geosciences, 97(4), 215–227. https://doi.org/10.1017/njg.2018.11

Li, X., Huang, G., & Kong, Q. (2018). Atmospheric Phase Delay Correction Of D-Insar Based On Sentinel-1a. The International Archives of the Photogrammetry, Remote Sensing and Spatial Information Sciences, XLII–3, 955–960. https://doi.org/10.5194/isprs-archives-XLII-3-955-2018

Lv, Y., Li, W., Wen, J., Xu, H., & Du, S. (2021). Population pattern and exposure under sea level rise: Low elevation coastal zone in the Yangtze River Delta, 1990–2100. Climate Risk Management, 33, 100348. https://doi.org/10.1016/j.crm.2021.100348

Minderhoud, P. S. J. (2019). The sinking mega-delta: Present and future subsidence of the Vietnamese Mekong delta. Utrecht Studies in Earth Sciences, 168. http://localhost/handle/1874/375843

Minderhoud, P. S. J., Middelkoop, H., Erkens, G., & Stouthamer, E. (2020). Groundwater extraction may drown mega-delta: Projections of extraction-induced subsidence and elevation of the Mekong delta for the 21st century. Environmental Research Communications, 2(1), 011005. https://doi.org/10.1088/2515-7620/ab5e21

Muis S, Verlaan M, Winsemius H C, et al. (2016) A global reanalysis of storm surges and extreme sea levels. Nature communications, 7(1): 1-12. https://doi.org/10.1038/ncomms11969

Nerem, R. S., Beckley, B. D., Fasullo, J. T., Hamlington, B. D., Masters, D., & Mitchum, G. T. (2018). Climate-change–driven accelerated sea-level rise detected in the altimeter era. Proceedings of the National Academy of Sciences, 115(9), 2022–2025. https://doi.org/10.1073/pnas.1717312115

Nicholls, R. J., Lincke, D., Hinkel, J., Brown, S., Vafeidis, A. T., Meyssignac, B., Hanson, S. E., Merkens, J.-L., & Fang, J. (2021). A global analysis of subsidence, relative sea-level change and coastal flood exposure. Nature Climate Change, 11(4), 338–342. https://doi.org/10.1038/s41558-021-00993-z

Peltier, W. R., Argus, D. F., & Drummond, R. (2015). Space geodesy constrains ice age terminal deglaciation: The global ICE-6G_C (VM5a) model. Journal of Geophysical Research: Solid Earth, 120(1), 450–487. https://doi.org/10.1002/2014JB011176

Pörtner, H.-O., Roberts, D. C., Masson-Delmotte, V., Zhai, P., Tignor, M., Poloczanska, E., Mintenbeck, K., Nicolai, M., Okem, A., & Petzold, J. (2019). IPCC special report on the ocean and cryosphere in a changing climate. IPCC Intergovernmental Panel on Climate Change: Geneva, Switzerland, 1(3).

Razvadauskas, F. V. (2019). Megacities: Developing Country Domination. London, UK: Euromonitor International.

Restrepo-Ángel, J. D., Mora-Páez, H., Díaz, F., Govorcin, M., Wdowinski, S., Giraldo-Londoño, L., Tosic, M., Fernández, I., Paniagua-Arroyave, J. F., & Duque-Trujillo, J. F. (2021). Coastal subsidence increases vulnerability to sea level rise over twenty first century in Cartagena, Caribbean Colombia. Scientific Reports, 11(1), 18873. https://doi.org/10.1038/s41598-021-98428-4

Ridder N N, Pitman A J, Westra S, et al. (2020). Global hotspots for the occurrence of compound events. Nature communications, 11(1): 1-10. https://doi.org/10.1038/s41467-020-19639-3

Rovere, A., Stocchi, P., & Vacchi, M. (2016). Eustatic and Relative Sea Level Changes. Current Climate Change Reports, 2(4), 221–231. https://doi.org/10.1007/s40641-016-0045-7

Shen, S.-L., & Xu, Y.-S. (2011). Numerical evaluation of land subsidence induced by groundwater pumping in Shanghai. Canadian Geotechnical Journal, 48(9), 1378–1392. https://doi.org/10.1139/t11-049

Shirzaei, M., & Bürgmann, R. (2018). Global climate change and local land subsidence exacerbate inundation risk to the San Francisco Bay Area. Science Advances, 4(3), eaap9234. https://doi.org/10.1126/sciadv.aap9234

Shirzaei, M., Freymueller, J., Törnqvist, T. E., Galloway, D. L., Dura, T., & Minderhoud, P. S. J. (2021). Measuring, modelling and projecting coastal land subsidence. Nature Reviews Earth & Environment, 2(1), 40–58. https://doi.org/10.1038/s43017-020-00115-x

Tessler, Z. D., Vörösmarty, C. J., Overeem, I., & Syvitski, J. P. M. (2018). A model of water and sediment balance as determinants of relative sea level rise in contemporary and future deltas. Geomorphology, 305, 209–220. https://doi.org/10.1016/j.geomorph.2017.09.040

Takagi, H., Esteban, M., Mikami, T., & Fujii, D. (2016a). Projection of coastal floods in 2050 Jakarta. Urban Climate, 17, 135–145. https://doi.org/10.1016/j.uclim.2016.05.003

Takagi, H., Esteban, M., Mikami, T., Fujii, D., & Kurobe, S. (2016b). Mechanisms Of Coastal Floods In Jakarta: The Need For Immediate Action Against Land Subsidence. The Proceedings of the ICOPMAS 2016, 3.

Vermeer, M.; Rahmstorf, S. (2009) Global sea level linked to global temperature. Proc. Natl. Acad. Sci. 106, 21527–21532. https://doi.org/10.1073/pnas.0907765106

Wang, B., Chen, S., Zhang, K., & Shen, J. (1995). Potential impacts of sea-level rise on the Shanghai area. Journal of Coastal Research, 151–166. https://www.jstor.org/stable/25735706

Wang, J., Gao, W., Xu, S., & Yu, L. (2012). Evaluation of the combined risk of sea level rise, land subsidence, and storm surges on the coastal areas of Shanghai, China. Climatic Change, 115(3–4), 537–558. https://doi.org/10.1007/s10584-012-0468-7

Wang, J., Yi, S., Li, M., Wang, L., & Song, C. (2018). Effects of sea level rise, land subsidence, bathymetric change and typhoon tracks on storm flooding in the coastal areas of Shanghai. Science of The Total Environment, 621, 228–234. https://doi.org/10.1016/j.scitotenv.2017.11.224

Xian, S., Yin, J., Lin, N., & Oppenheimer, M. (2018). Influence of risk factors and past events on flood resilience in coastal megacities: Comparative analysis of NYC and Shanghai. Science of The Total Environment, 610–611, 1251–1261. https://doi.org/10.1016/j.scitotenv.2017.07.229

Xu, Y.-S., Ma, L., Du, Y.-J., & Shen, S.-L. (2012). Analysis of urbanisation-induced land subsidence in Shanghai. Natural Hazards, 63(2), 1255–1267. https://doi.org/10.1007/s11069-012-0220-7

Xue, Y.-Q., Zhang, Y., Ye, S.-J., Wu, J.-C., & Li, Q.-F. (2005). Land subsidence in China. Environmental Geology, 48(6), 713–720. https://doi.org/10.1007/s00254-005-0010-6

Yan, B., Li, S., Wang, J., Ge, Z., & Zhang, L. (2016). Socio-economic vulnerability of the megacity of Shanghai (China) to sea-level rise and associated storm surges. Regional Environmental Change, 16(5), 1443–1456. https://doi.org/10.1007/s10113-015-0878-y

Yang Y, Yin J, Zhang W, et al. (2021). Modeling of a compound flood induced by the levee breach at Qianbujing Creek, Shanghai, during Typhoon Fitow. Natural Hazards and Earth System Sciences, 21(11): 3563-3572. https://doi.org/10.5194/nhess-21-3563-2021

Ye, S., Xue, Y., Wu, J., Yan, X., & Yu, J. (2016). Progression and mitigation of land subsidence in China. Hydrogeology Journal, 24(3), 685–693. https://doi.org/10.1007/s10040-015-1356-9

Yin, J., Yu, D., Yin, Z., Wang, J., & Xu, S. (2013). Modelling the combined impacts of sea-level rise and land subsidence on storm tides induced flooding of the Huangpu River in Shanghai, China. Climatic Change, 119(3–4), 919–932. https://doi.org/10.1007/s10584-013-0749-9

Yin, J., Yu, D., Yin, Z., Wang, J., & Xu, S. (2015). Modelling the anthropogenic impacts on fluvial flood risks in a coastal mega-city: A scenario-based case study in Shanghai, China. Landscape and Urban Planning, 136, 144–155. https://doi.org/10.1016/j.landurbplan.2014.12.009

Yin, J., Jonkman, S., Lin, N., Yu, D., Aerts, J., Wilby, R., Pan, M., Wood, E., Bricker, J., Ke, Q., Zeng, Z., Zhao, Q., Ge, J., & Wang, J. (2020). Flood Risks in Sinking Delta Cities: Time for a Reevaluation? Earth's Future, 8(8). https://doi.org/10.1029/2020EF001614

Yin, J., Qing Zhao, & Dapeng Yu. (2019). Long-term flood-hazard modeling for coastal areas using InSAR measurements and a hydrodynamic model: The case study of Lingang New City, Shanghai. Journal of Hydrology, 571, 593-604. https://doi.org/10.1016/j.jhydrol.2019.02.015

Yin, J., Lin, N., Yang, Y., Pringle, W. J., Tan, J., Westerink, J. J., & Yu, D. (2021). Hazard Assessment for Typhoon- Induced Coastal Flooding and Inundation in Shanghai, China. Journal of Geophysical Research: Oceans, 126(7). https://doi.org/10.1029/2021JC017319

Yu, L., Yang, T., Zhao, Q., Liu, M., & Pepe, A. (2017). The 2015–2016 Ground Displacements of the Shanghai Coastal Area Inferred from a Combined COSMO-SkyMed/Sentinel-1 DInSAR Analysis. Remote Sensing, 9(11), 1194. https://doi.org/10.3390/rs9111194

Yuill, B., Lavoie, D., & Reed, D. J. (2009). Understanding subsidence processes in coastal Louisiana. Journal of Coastal Research, 10054, 23–36. https://www.jstor.org/stable/25737466

Zhao, Q., Pepe, A., Gao, W., Lu, Z., Bonano, M., He, M. L., Wang, J., & Tang, X. (2015). A DInSAR Investigation of the Ground Settlement Time Evolution of Ocean-Reclaimed Lands in Shanghai. IEEE Journal of Selected Topics in Applied Earth Observations and Remote Sensing, 8(4), 1763–1781. https://doi.org/10.1109/JSTARS.2015.2402168

Zhao, Q., Ma, G., Wang, Q., Yang, T., Liu, M., Gao, W., Falabella, F., Mastro, P., & Pepe, A. (2019). Generation of long-term InSAR ground displacement time-series through a novel multi-sensor data merging technique: The case study of the Shanghai coastal area. ISPRS Journal of Photogrammetry and Remote Sensing, 154, 10–27. https://doi.org/10.1016/j.isprsjprs.2019.05.005

Zhang, Y., Wu, J., Xue, Y., Wang, Z., Yao, Y., Yan, X., & Wang, H. (2015). Land subsidence and uplift due to long-term groundwater extraction and artificial recharge in Shanghai, China. Hydrogeology Journal, 23(8), 1851–1866. https://doi.org/10.1007/s10040-015-1302-x